

## Article

# Recyclable Fe<sub>3</sub>O<sub>4</sub> Nanoparticles Catalysts for Aza-Michael Addition of Acryl Amides by Magnetic Field

Zhen-Xing Li <sup>1,\*†</sup>, Dan Luo <sup>1,†</sup>, Ming-Ming Li <sup>1,†</sup>, Xiao-Fei Xing <sup>1</sup>, Zheng-Zheng Ma <sup>1</sup> and Hao Xu <sup>2,\*</sup>

<sup>1</sup> State Key Laboratory of Heavy Oil Processing, Institute of New Energy, China University of Petroleum (Beijing), Beijing 102249, China; luodan@iccas.ac.cn (D.L.); limingming\_cup@163.com (M.-M.L.); xingxiaofei\_cup@126.com (X.-F.X.); mzz0430@163.com (Z.-Z.M.)

<sup>2</sup> Institute of Fine Chemistry and Engineering, Henan Engineering Laboratory of Flame-Retardant and Functional Materials, College of Chemistry and Chemical Engineering, Henan University, Kaifeng 475004, China

\* Correspondence: lizx@cup.edu.cn (Z.-X.L.); xuhao@henu.edu.cn (H.X.)

† These authors contributed equally to this work.

Received: 20 June 2017; Accepted: 18 July 2017; Published: 20 July 2017

**Abstract:** A nanostructure-based catalytic system has the advantages of both homogeneous and heterogeneous catalysis. It is of great significance to develop the sustainable and green process of homogeneous catalytic reaction. We report a novel, efficient and recyclable magnetic Fe<sub>3</sub>O<sub>4</sub> nanoparticles-catalyzed aza-Michael addition reaction of acryl amides, and the magnetic nanoparticles catalysts can be recovered by external magnetic field. Both primary amine and secondary amine can react with various acryl amides providing a good output to target products successfully at room temperature. Further experiments reveal that the magnetic Fe<sub>3</sub>O<sub>4</sub> nanoparticles-based catalyst shows excellent yields, which can be recycled 10 times, and, at the same time, it maintains a high catalytically activity. In this catalytic system, the tedious separation procedures are replaced by external magnetic field, which gives us a different direction for choosing a catalyst in a nanostructure-based catalytic system.

**Keywords:** Fe<sub>3</sub>O<sub>4</sub> nanoparticle; aza-Michael addition; recyclable catalyst; acryl amides; magnetic field; heterogeneous catalysis

## 1. Introduction

Environmental pollution caused by man-made waste and the decrease of natural resources is the main threat that has caught the attention of the whole world. The growing population needs more resources and naturally generates more waste. Land, air and fresh water, which are necessary for human life, all get affected by the release of chemical waste. For the sake of reduction in the harmful effects of the pollution and resource depletion, the best remedy is to develop the sustainable and atom-economic chemical process. This process can be improved upon by careful selection of starting materials and a catalytic system. Homogeneous catalysis is studied extensively as a powerful catalytic system, because of its special capabilities including high efficiency, flexible structures, high catalytic selectivity and activity, and so on. Nevertheless, the homogeneous catalyst is often difficult to isolate from reaction product, because both of the catalyst, reactants and products are same phase, which effects its extensive appliance [1]. Therefore, it is not only an environmentally-friendly but an atom-economic chemical process. The heterogeneous catalysis is distinguished from homogeneous catalysis by the different phases present during reaction. The main advantage of using a heterogeneous catalyst is the

relative ease of catalyst separation from the product. Therefore, the catalyst can be recycled and achieve the continuous chemical processes. The creation of a catalytic system, which has advantages of both homogeneous and heterogeneous catalysis, is of great significance. A nanostructure-based catalytic system provides an opportunity to meet the requirements, because the nanoparticles show not only large surface areas, but also tunable exposed surface, and high dispersity in the solvent [2].

Recently, many efforts have been made to use noble metal nanoparticles as catalysts in a homogeneous catalytic system, based on rationale design [3–17], e.g., cyclization reactions catalyzed by Pt nanoparticles [18], Heck coupling reactions and Ullmann coupling reactions of chlorobenzene catalyzed by Pd nanoparticles catalysts [19], and Heck and Suzuki reactions catalyzed by Pd nanoparticles [20], cycloisomerizations of enynes catalyzed by Au/CeO<sub>2</sub> nanocubes [21], and so on. However, the metal oxide has been more or less neglected. Compared with noble metal nanoparticles catalysts, the metal oxide is low-cost, low-toxicity and has tunable properties. Hence, a metal oxide nanoparticles-based catalytic system has great potential inorganic synthesis.

The Michael addition reaction is of such importance in inorganic synthesis [22]; thus, carbon-heteroatom and carbon-carbon bonds can be formed by this atom-economy and efficiency approach [23–27]. Especially, the aza-Michael addition reaction of acryl amides is a widely used in research and industry owing to its importance for several pharmaceutical products or important pharmaceutical intermediates, which can also be transformed into a large range of biologically active molecules under further treatment [28–30]. In traditional organic synthesis, the Michael addition reaction is catalyzed by strong bases, and the catalysts are quite difficult to recover and recycle, and moreover, the undesirable side reactions are unavoidable [31–34]. Therefore, this process is not sustainable and green chemistry. Herein, we report a novel, efficient and recyclable magnetic Fe<sub>3</sub>O<sub>4</sub> nanoparticles-catalyzed aza-Michael addition reaction of acryl amides with amines, and the magnetic Fe<sub>3</sub>O<sub>4</sub> nanoparticle catalysts can easily be recovered by external magnetic field.

## 2. Results and Discussion

Thermal decomposition of metal organic precursors is one of the best ways to prepare the high-quality monodisperse nanoparticles in high-boiling point solvent [35–40], such as, metal acetylacetonates [35,36], metal carbonyls, etc. The monodisperse Fe<sub>3</sub>O<sub>4</sub> nanoparticles with good crystallinity and uniform size is obtained by thermal decomposition of the iron acetylacetonates dissolved in 1-octadecene at 300 °C using oleic acid and oleyl amine as surfactants under argon atmosphere. The size and shape of the obtained Fe<sub>3</sub>O<sub>4</sub> nanoparticles were measured through using transmission electron microscopy (TEM). Figure 1 is representative images of obtained Fe<sub>3</sub>O<sub>4</sub> nanoparticles. The perfectly spherical Fe<sub>3</sub>O<sub>4</sub> nanoparticles are highly uniform, with diameter of 13 nm (Figure 1a). The high uniformity of these Fe<sub>3</sub>O<sub>4</sub> nanoparticles allows the formation of nanoarrays arranged with long range order. After slow evaporation of a concentrated Fe<sub>3</sub>O<sub>4</sub> nanoparticles solution in hexane, the super lattice of Fe<sub>3</sub>O<sub>4</sub> nanoparticles are formed on the TEM grid (Figure 1b). The high-resolution TEM (HRTEM) image show that Fe<sub>3</sub>O<sub>4</sub> nanoparticle is of single crystalline nature enclosed by the (111) plane and the surfaces are perfect without any sheathed amorphous phase (Figure 1c). The selected area electron diffraction (SAED) pattern (Figure 1d) further confirms that the spherical Fe<sub>3</sub>O<sub>4</sub> nanoparticle is single crystalline nature. The SAED pattern exhibits that the *d* space is 0.24, 0.21, 0.17 and 0.13 nm, which correspond to the (222), (400), (422), and (533) planes of the standard cubic structure of Fe<sub>3</sub>O<sub>4</sub> pattern.

The crystallinity and structure of the Fe<sub>3</sub>O<sub>4</sub> nanoparticles are also confirmed by powder X-ray diffraction (XRD). The XRD pattern is illustrated in Figure 2. The diffraction peaks are indexed to (220), (311), (400), (511) and (440) reflections, corresponding to a cubic structure with lattice constants in the range of 0.5421–0.5432 nm (JCPDS card no. 11-0614, *a* = 0.83963 nm, space group *Fd-3m*). The relative intensity and peak position of all diffraction peaks are in good agreement with standard powder diffraction data, and no crystallized precursor is observed in the XRD pattern. The broadening of the reflections distinctly indicates the intrinsic nature of nanocrystals, which agrees well with the TEM results.

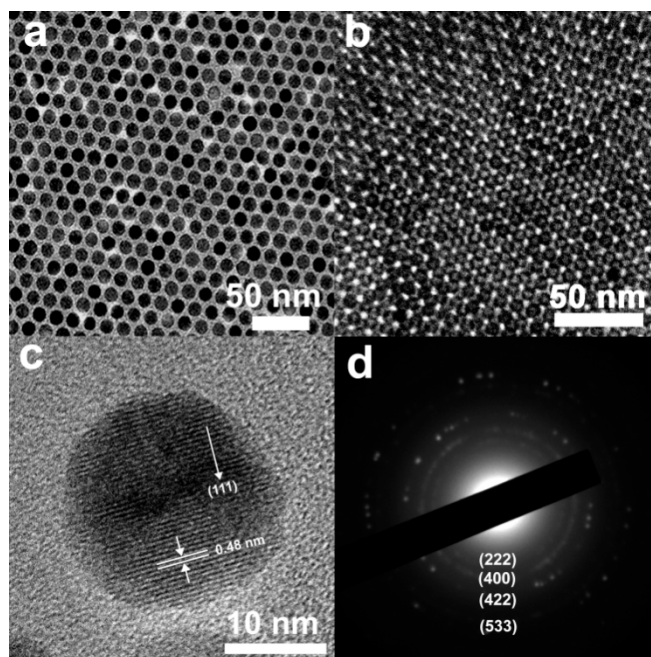


**Figure 1.** (a) Transmission electron microscopy (TEM) image of the prepared  $\text{Fe}_3\text{O}_4$  nanoparticles; (b) The superlattice of  $\text{Fe}_3\text{O}_4$  nanoparticles are formed on the TEM grid; (c) High-resolution TEM (HRTEM) image of the prepared  $\text{Fe}_3\text{O}_4$  nanoparticles; (d) Selected area electron diffraction (SAED) pattern of the prepared  $\text{Fe}_3\text{O}_4$  nanoparticles.

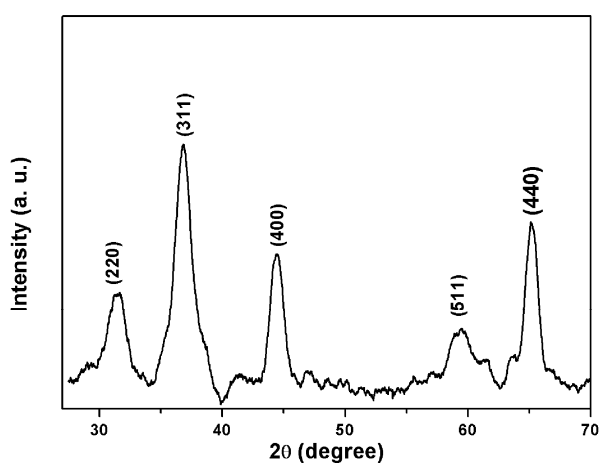


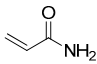
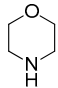
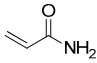
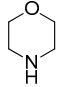
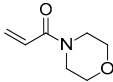
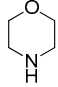
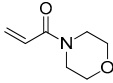
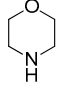
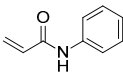
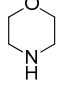
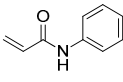
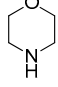
**Figure 2.** Powder X-ray diffraction (XRD) of the prepared  $\text{Fe}_3\text{O}_4$  nanoparticles.

The aza-Michael addition reaction of acryl amides is significant for preparing kinds of  $\beta$ -amino carbonyl compounds from readily manufactured raw materials in a sustainable and clean method [41–46]. Recently, the researches in aza-Michael addition by the imidazolium-based polymer [47], enzymes [48–51], and room-temperature ionic liquids (RTILs) have given a novelty way to achieve the important  $\beta$ -amino carbonyl derivatives [28]. These methods definitely have excellent potential as powerful tools which can build multiple molecules with different acryl amides, and in the meantime provide new catalytic cascade reaction sequences. Even if basic studies have effectively expanded the range of substrates for aza-Michael addition reaction, the relatively difficulty to separate the product and reuse the catalysts in the reaction have effected its application a lot. Moreover, the magnetic nanostructure-based catalyst is a prospective way to improve this situation effectively. In contrast, the smooth instances of magnetic nanostructure-based catalysts that display

creditable catalytic reactivity are as yet unusual in practice. We design a magnetic nanoparticles-based catalytic system, by using the magnetic  $\text{Fe}_3\text{O}_4$  nanoparticles as catalysts, and the external magnetic field segregate catalyst readily with the reaction products by an external magnetic field.

We investigate the aza-Michael addition reaction of various substituents on N position of acryl amides catalyzed by the magnetic  $\text{Fe}_3\text{O}_4$  nanoparticles. The reactions are carried out by using dichloromethane as the solvent normal pressure of atmosphere air at room temperature and the result is presented in Table 1. The magnetic  $\text{Fe}_3\text{O}_4$  nanoparticles show excellent catalytic performance in the aza-Michael addition reaction, which can significantly enhance the yield of the desired product. The reactivity of Michael acceptors is affected by the substituent on the N position of acryl amide. The acrylamide and 1-morpholinoprop-2-en-1-one show a low reaction rate and yield (Table 1, entries 1, 3), and the *N*-phenylacrylamide exhibits higher the reaction rate and yield (Table 1, entries 5). The isolated yields are 38.1, 36.2 and 39.6, respectively. In contrast, under the magnetic  $\text{Fe}_3\text{O}_4$  nanoparticles-catalyzed conditions, the acrylamide and 1-morpholinoprop-2-en-1-one are efficient Michael acceptors to give the corresponding products in 89% and 85.2% yields (Table 1, entries 2, 4). In addition, it is most significant that the isolated yield of *N*-phenylacrylamide reached up to 93.2% (Table 1, entry 6). It is worth mentioning that the magnetic  $\text{Fe}_3\text{O}_4$  nanoparticles significantly improve the reaction rate and yield of acryl amide.

**Table 1.** Influence of the  $\text{Fe}_3\text{O}_4$  nanoparticles on the aza-Michael addition of various substituent on N position of acryl amides with morpholine. <sup>a</sup>

Entry	Acryl Amide	Amine	Catalyst	Yield (%) <sup>b</sup>
1			-	38.1
2			$\text{Fe}_3\text{O}_4$ nanoparticles	89.0
3			-	36.2
4			$\text{Fe}_3\text{O}_4$ nanoparticles	85.2
5			-	39.6
6			$\text{Fe}_3\text{O}_4$ nanoparticles	93.2

<sup>a</sup> Reaction conditions: acryl amides (2 mmol), amines (2 mmol), and catalyst (10 mol %) in 1 mL of  $\text{CH}_2\text{Cl}_2$  for 24 h at room temperature in a Schlenk tube; <sup>b</sup> Isolated yield.

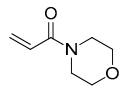
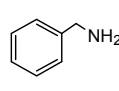
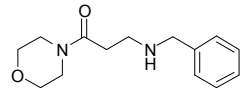
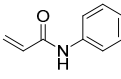
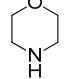
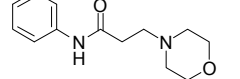
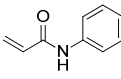
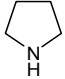
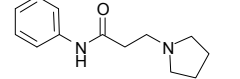
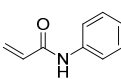
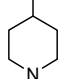
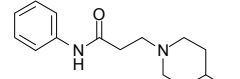
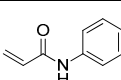
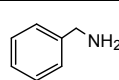
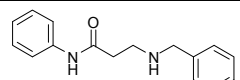
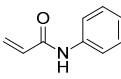
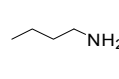
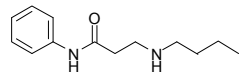
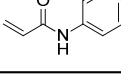
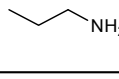
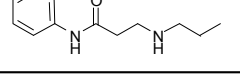
Such a catalytic ability of the magnetic  $\text{Fe}_3\text{O}_4$  nanoparticles-based catalyst is not novel to amines, other common amines substrates can be performed too. In addition, all of them performed high isolated yield (Table 2, entries 1–16). The secondary amines such as morpholine (Table 2, entries 1, 7 and 13), pyrrolidine (Table 2, entries 2, 8 and 14), 2-methylpiperidine (Table 2, entries 3 and 9), 4-methylpiperidine (Table 2, entries 4, 10 and 15) and 1-ethylpiperazine (Table 2, entries 5 and 11) are efficient Michael donors and the yield is more than 80%. Furthermore, the primary amine (phenylmethanamine) also exhibit high reaction rate and yield, and the isolated yields are 80.2, 90.1 and 80.1, respectively (Table 2, entries 6, 12 and 16). In addition, this aza-Michael

addition reaction can also be carried out on the acyclic amines. The n-butylamine and n-propylamine (Table 2, entries 17 and 18) have been tested and the isolated yields are 78.6% and 77.9%, respectively. The substituted amides and acyclic secondary amines cannot be catalyzed by the  $\text{Fe}_3\text{O}_4$  nanoparticles in a reaction system.

**Table 2.** The magnetic  $\text{Fe}_3\text{O}_4$  nanoparticles-catalyzed aza-Michael addition of acryl amides with various amines. <sup>a</sup>

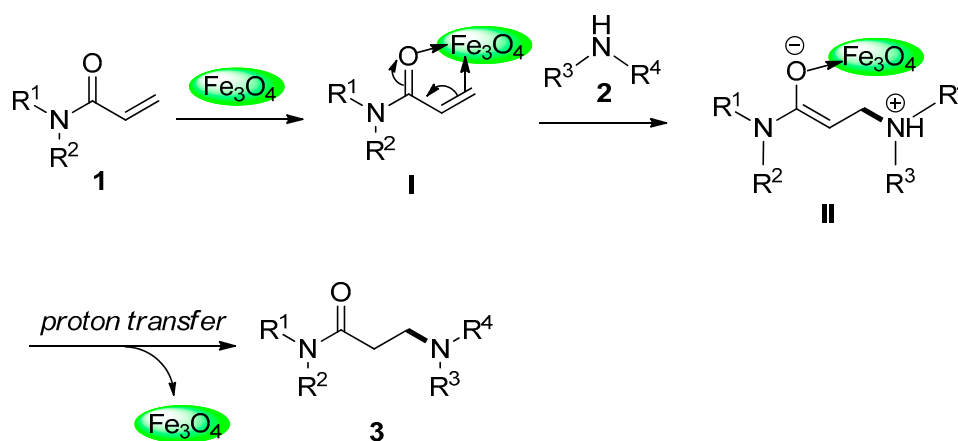
Entry	Acryl Amides	Amine	Product	Yield (%) <sup>b</sup>
1				89.0
2				90.6
3				90.4
4				91.7
5				90.1
6				80.2
7				85.2
8				86.9
9				84.3
10				85.6
11				80.2

Table 2. Cont.

Entry	Acryl Amides	Amine	Product	Yield (%) <sup>b</sup>
12				90.1
13				93.2
14				81.2
15				84.6
16				80.1
17				78.6
18				77.9

<sup>a</sup> Reaction conditions: acryl amides (2 mmol), amines (2 mmol), and catalyst (10 mol %) in 1 mL of CH<sub>2</sub>Cl<sub>2</sub> for 24 h at room temperature in a Schlenk tube; <sup>b</sup> Isolated yield.

According to all the experimental results, a feasible mechanism for Fe<sub>3</sub>O<sub>4</sub> nanoparticles-catalyzed aza-Michael addition of acryl amide with amines is proposed in Scheme 1. Coordination of **1** with Fe<sub>3</sub>O<sub>4</sub> nanoparticles leads to **I**; amine **2** added to the activated double bond to form **II**; Proton transfer of **II** gives product **3** and leaves Fe<sub>3</sub>O<sub>4</sub> nanoparticles.



**Scheme 1.** A possible mechanism for Fe<sub>3</sub>O<sub>4</sub> nanoparticles-catalyzed aza-Michael addition of acryl amides with amines.

It is generally agreed that the recovery of the catalyst system is the main factor to determine whether it has potential large-scale application in industry or not. To illustrate the recycling performance of the magnetic Fe<sub>3</sub>O<sub>4</sub> nanoparticles-based catalyst, the model reaction of



N-phenylacrylamide with morpholine is chosen to investigate the reusability of the magnetic  $\text{Fe}_3\text{O}_4$  nanoparticles-based catalyst. The magnetic  $\text{Fe}_3\text{O}_4$  nanoparticles can be segregated readily with the reaction products by external magnetic field (Figure 3), which shows good recyclability. Moreover, the recycled catalyst shows the magnetic  $\text{Fe}_3\text{O}_4$  nanoparticles are extremely stable with excellent catalytic activity of 86.3% after the tenth reuse (Figure 4). The isolated yields from the first to tenth catalytic reaction are 93.2, 92.6, 91.4, 90.6, 90.6, 89.5, 88.6, 88.6, 87.4 and 86.3, respectively. Because the outside of the  $\text{Fe}_3\text{O}_4$  nanoparticles has been overlapped fractionally with organic compounds, the catalytic activity can decline mildly. In addition, the TEM image and powder XRD of the  $\text{Fe}_3\text{O}_4$  nanoparticles after the catalytic reaction does not exhibit any appreciable aggregation or leaching (Figures S1 and S2). Based on the above experimental data, no catalytically active species have been leached from  $\text{Fe}_3\text{O}_4$  nanoparticles in the reactive process, and the catalytically active species are  $\text{Fe}_3\text{O}_4$  nanoparticles.

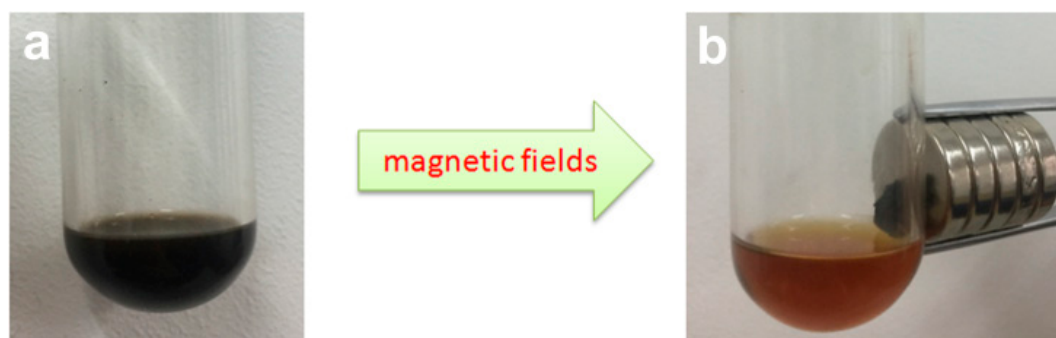


**Figure 3.** The magnetic  $\text{Fe}_3\text{O}_4$  nanoparticles can be recovered from the reaction products by external magnetic field. (a) the reaction products and  $\text{Fe}_3\text{O}_4$  nanoparticles before the external magnetic field; (b) the reaction products and  $\text{Fe}_3\text{O}_4$  nanoparticles after the external magnetic field.

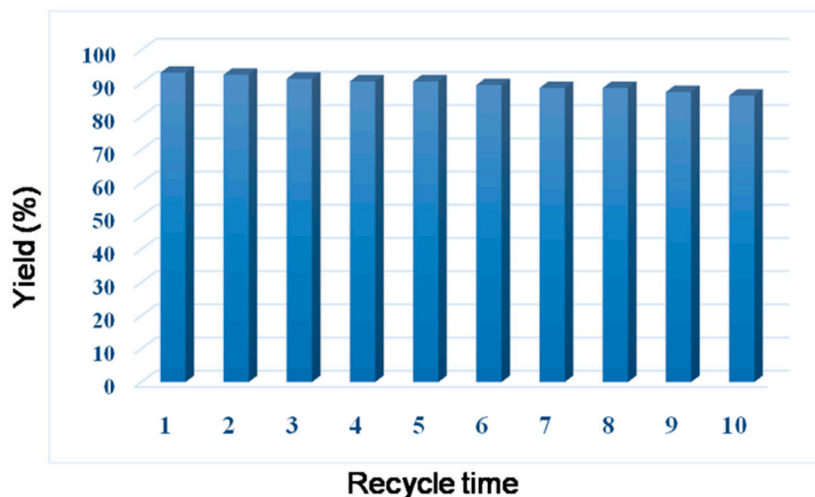


**Figure 4.** The reuses of magnetic  $\text{Fe}_3\text{O}_4$  nanoparticles on the aza-Michael addition of N-phenylacrylamide with morpholine.

### 3. Experimental

#### 3.1. Synthesis of Magnetic $\text{Fe}_3\text{O}_4$ nanoparticles

The magnetic  $\text{Fe}_3\text{O}_4$  nanoparticles were prepared as previously reported involving two-steps: synthesis  $\text{Fe}_3\text{O}_4$  seeds and growth of  $\text{Fe}_3\text{O}_4$  nanoparticles [35].  $\text{Fe}(\text{acac})_3$  (2 mmol), oleylamine (6 mmol), oleic acid (6 mmol), 1,2-hexadecanediol (10 mmol) and benzyl ether (20 mL) were added in a three-neck round bottom flask, then heated to 200 °C for 2 h. Then the mixture was heated to reflux at 300 °C

for 1 h under argon flow. The reaction was stopped by cooling to room temperature. The obtained  $\text{Fe}_3\text{O}_4$  seeds were washed thrice with adding appropriate amount of ethanol and dispersed in hexane.  $\text{Fe}(\text{acac})_3$  (4 mmol), benzyl ether (20 mL), oleic acid (2 mmol), 1,2-hexadecanediol (20 mmol) and oleylamine (2 mmol) added in a three-neck round bottom flask, and then magnetically stirred under argon flow. 80 mg of  $\text{Fe}_3\text{O}_4$  seeds were added and then the mixture was heated to 120 °C for 1 h and then heated to 200 °C for 2 h. After that, the mixture was further heated to 300 °C for 60 min under argon flow. The obtained  $\text{Fe}_3\text{O}_4$  nanoparticles were washed thrice by adding an appropriate amount of ethanol and dispersed in hexane.

### 3.2. Characterization

The powder X-ray diffraction (XRD) patterns were recorded on a RigakuD/MAX-2000 diffractometer (Rigaku Corporation, Tokyo, Japan) using  $\text{Cu-K}\alpha$  radiation ( $\lambda = 1.5406 \text{ \AA}$ ). The transmission electron microscopy (TEM) observations were performed on a Philips Tecnai F20 FEG-TEM (FEI Company, Hillsboro, OR, USA) operated at 200 kV. The FTIR absorption spectrum was recorded on a Bruker spectrometer.

### 3.3. Representative Procedure for Catalytic Reactions

A mixture of acryl amides (2 mmol), amines (2 mmol) and the magnetic  $\text{Fe}_3\text{O}_4$  nanoparticles (10 mol %) was stirred in 1 mL of  $\text{CH}_2\text{Cl}_2$  for 24 h at 32 °C in a Schlenk tube. The reaction mixture was extracted with ethyl acetate when the reaction was completed (monitored by Thin Layer Chromatography (TLC)). The resulting crude product was purified with column chromatography by using petroleum ether/ethyl acetate or methanol/ethyl acetate as the eluent. The resulting products were characterized by  $^1\text{H}$  NMR. The catalyst used in the reaction was segregated with external magnetic field and then used in subsequent reactions without further processing.

1. 3-morpholinopropanamide (Table 2, entry 1).  $^1\text{H}$  NMR (600 MHz,  $\text{CDCl}_3$ ) (ppm):  $\delta$  7.92 (s, 1H), 5.64 (s, 1H), 3.90–3.80 (m, 2H), 3.72 (s, 2H), 2.41–2.63 (m, 8H).
2. 3-(pyrrolidin-1-yl)propanamide (Table 2, entry 2).  $^1\text{H}$  NMR (600 MHz,  $\text{CDCl}_3$ ) (ppm):  $\delta$  8.00 (s, 1H), 5.38 (s, 1H), 2.86 (t,  $J = 6.2 \text{ Hz}$ , 2H), 2.70 (s, 4H), 2.52 (t,  $J = 6.2 \text{ Hz}$ , 2H), 1.91–1.80 (m, 4H).
3. 3-(2-methylpiperidin-1-yl)propanamide (Table 2, entry 3).  $^1\text{H}$  NMR (600 MHz,  $\text{CDCl}_3$ ) (ppm):  $\delta$  8.38 (s, 1H), 5.56 (s, 1H), 3.72 (q,  $J = 7.0 \text{ Hz}$ , 2H), 3.40 (d,  $J = 11.9 \text{ Hz}$ , 2H), 2.81 (t,  $J = 11.0 \text{ Hz}$ , 2H), 1.89 (s, 1H), 1.67 (d,  $J = 12.7 \text{ Hz}$ , 2H), 1.49 (d,  $J = 6.5 \text{ Hz}$ , 2H), 1.3 (t,  $J = 7.0 \text{ Hz}$ , 2H), 1.12 (d,  $J = 6.3 \text{ Hz}$ , 3H).
4. 3-(4-methylpiperidin-1-yl)propanamide (Table 2, entry 4).  $^1\text{H}$  NMR (600 MHz,  $\text{CDCl}_3$ ) (ppm):  $\delta$  8.47 (s, 1H), 5.48 (s, 1H), 3.73 (q,  $J = 7.0 \text{ Hz}$ , 2H), 2.94 (d,  $J = 11.4 \text{ Hz}$ , 2H), 2.62–2.56 (m, 2H), 2.40 (t,  $J = 6.0 \text{ Hz}$ , 2H), 1.98 (t,  $J = 12.3 \text{ Hz}$ , 2H), 1.68 (d,  $J = 13.4 \text{ Hz}$ , 1H), 1.25 (t,  $J = 8.3 \text{ Hz}$ , 2H), 0.94 (d,  $J = 6.5 \text{ Hz}$ , 3H).
5. 3-(4-ethylpiperazin-1-yl)propanamide (Table 2, entry 5).  $^1\text{H}$  NMR (600 MHz,  $\text{CDCl}_3$ ) (ppm):  $\delta$  8.09 (s, 1H), 5.47 (s, 1H), 2.68–2.60 (m, 3H), 2.47–2.37 (m, 11H), 1.10 (t,  $J = 7.2 \text{ Hz}$ , 3H).
6. 3-(benzylamino)propanamide (Table 2, entry 6).  $^1\text{H}$  NMR (600 MHz,  $\text{CDCl}_3$ ) (ppm):  $\delta$  7.49 (s, 1H), 7.23–7.25 (m, 4H), 6.26 (s, 1H), 3.71 (s, 4H), 1.33 (d,  $J = 6.9 \text{ Hz}$ , 2H), 1.23 (t,  $J = 6.7 \text{ Hz}$ , 2H).
7. 3-morpholino-1-morpholinopropan-1-one (Table 2, entry 7).  $^1\text{H}$  NMR (600 MHz,  $\text{CDCl}_3$ ) (ppm):  $\delta$  3.71 (t,  $J = 4.5 \text{ Hz}$ , 4H), 3.68–3.60 (m, 2H), 3.60 (s, 4H), 3.45 (d,  $J = 4.7 \text{ Hz}$ , 2H), 2.74 (t,  $J = 7.4 \text{ Hz}$ , 2H), 2.52 (d,  $J = 19.6 \text{ Hz}$ , 4H), 2.36 (s, 4H).
8. 1-morpholino-3-(pyrrolidin-1-yl)propan-1-one (Table 2, entry 8).  $^1\text{H}$  NMR (600 MHz,  $\text{CDCl}_3$ ) (ppm):  $\delta$  3.71–3.60 (m, 6H), 3.57 (d,  $J = 4.7 \text{ Hz}$ , 2H), 2.93 (t,  $J = 7.3 \text{ Hz}$ , 6H), 2.04 (s, 4H).
9. 3-(2-methylpiperidin-1-yl)-1-morpholinopropan-1-one (Table 2, entry 9).  $^1\text{H}$  NMR (600 MHz,  $\text{CDCl}_3$ ) (ppm):  $\delta$  3.70 (q,  $J = 7.0 \text{ Hz}$ , 4H), 3.41 (d,  $J = 12.7 \text{ Hz}$ , 4H), 2.79 (t,  $J = 11.1 \text{ Hz}$ , 2H), 2.52 (d,  $J = 7.8 \text{ Hz}$ , 2H), 2.41 (s, 2H), 1.85 (s, 1H), 1.68 (s, 1H), 1.46 (d,  $J = 9.8 \text{ Hz}$ , 2H), 1.42 (t,  $J = 7.0 \text{ Hz}$ , 2H), 1.06 (s, 3H).



10. 3-(4-methylpiperidin-1-yl)-1-morpholinopropan-1-one (Table 2, entry 10).  $^1\text{H}$  NMR (600 MHz,  $\text{CDCl}_3$ ) (ppm):  $\delta$  3.76–3.67 (m, 1H), 3.67–3.58 (m, 4H), 3.53–3.45 (m, 5H), 2.93 (d,  $J$  = 11.5 Hz, 2H), 2.79–2.71 (m, 2H), 2.63–2.55 (m, 2H), 2.06 (t,  $J$  = 11.0 Hz, 2H), 1.96 (s, 1H), 1.65 (d,  $J$  = 13.5 Hz, 2H), 0.93 (d,  $J$  = 6.5 Hz, 3H).
11. 3-(4-ethylpiperazin-1-yl)-1-morpholinopropan-1-one (Table 2, entry 11).  $^1\text{H}$  NMR (600 MHz,  $\text{CDCl}_3$ ) (ppm):  $\delta$  3.69–3.68 (m, 6H), 3.49 (d,  $J$  = 5.0 Hz, 2H), 2.53 (d,  $J$  = 8.0 Hz, 2H), 2.45–2.29 (m, 12H), 1.11 (t,  $J$  = 7.2 Hz, 3H).
12. 3-(benzylamino)-1-morpholinopropan-1-one (Table 2, entry 12).  $^1\text{H}$  NMR (600 MHz,  $\text{CDCl}_3$ ) (ppm):  $\delta$  7.49 (d,  $J$  = 6.2 Hz, 5H), 4.12 (s, 2H), 3.64 (d,  $J$  = 3.6 Hz, 4H), 3.54 (s, 4H), 2.97 (s, 2H), 2.03 (s, 2H), 1.24 (s, 1H).
13. 3-morpholin-4-yl-*N*-phenyl-propionamide (Table 2, entry 13).  $^1\text{H}$  NMR (400 MHz,  $\text{CDCl}_3$ ) (ppm):  $\delta$  11.31 (s, 1H), 7.53 (d,  $J$  = 8.6 Hz, 2H), 7.30 (d,  $J$  = 9.9 Hz, 2H), 7.07 (t,  $J$  = 7.4 Hz, 1H), 3.04 (d,  $J$  = 11.7 Hz, 2H), 2.72–2.64 (m, 4H), 2.55–2.47 (m, 2H), 2.07 (t,  $J$  = 10.8 Hz, 4H).
14. *N*-phenyl-3-pyrrolidin-1-yl-propionamide (Table 2, entry 14).  $^1\text{H}$  NMR (600 MHz,  $\text{CDCl}_3$ ) (ppm):  $\delta$  9.97 (s, 1H), 7.66 (d,  $J$  = 7.9 Hz, 2H), 7.29 (d,  $J$  = 7.0 Hz, 2H), 7.09 (t,  $J$  = 7.3 Hz, 1H), 3.73 (q,  $J$  = 7.0 Hz, 2H), 3.11 (t,  $J$  = 6.5 Hz, 2H), 2.08 (s, 4H), 1.25 (t,  $J$  = 7.0 Hz, 4H).
15. 3-(4-methyl-piperidin-1-yl)-*N*-phenyl-propionamide (Table 2, entry 15).  $^1\text{H}$  NMR (400 MHz,  $\text{CDCl}_3$ ) (ppm):  $\delta$  10.76 (s, 1H), 7.53 (d,  $J$  = 7.9 Hz, 2H), 7.32 (t,  $J$  = 7.8 Hz, 2H), 7.08 (t,  $J$  = 7.4 Hz, 1H), 3.82 (s, 2H), 2.87 (d,  $J$  = 23.3 Hz, 2H), 2.86 (d,  $J$  = 37.1 Hz, 2H), 2.71 (d,  $J$  = 29.6, 23.8 Hz, 2H), 1.74 (m, 1H), 1.25 (s, 4H), 0.86 (s, 3H).
16. 3-benzylamino-*N*-phenyl-propionamide (Table 2, entry 16).  $^1\text{H}$  NMR (600 MHz,  $\text{CDCl}_3$ ) (ppm):  $\delta$  10.44 (s, 1H), 7.52 (d,  $J$  = 7.8 Hz, 2H), 7.41–7.25 (m, 7H), 7.07 (s, 1H), 3.88 (s, 2H), 2.97 (m, 2H), 2.59–2.51 (m, 2H), 1.94 (d,  $J$  = 6.7 Hz, 1H).
17. 3-butyl-*N*-phenyl-propionamide (Table 2, entry 17).  $^1\text{H}$  NMR (600 MHz,  $\text{CDCl}_3$ ) (ppm):  $\delta$  10.51 (s, 1H), 7.45 (d,  $J$  = 7.9 Hz, 2H), 7.24 (m, 2H), 6.97 (t,  $J$  = 7.4 Hz, 1H), 2.95 (m, 2H), 2.57 (t,  $J$  = 7.0 Hz, 4H), 1.37 (d,  $J$  = 8.6 Hz, 4H), 1.23 (s, 1H), 0.78 (s, 3H).
18. 3-propyl-*N*-phenyl-propionamide (Table 2, entry 18).  $^1\text{H}$  NMR (600 MHz,  $\text{CDCl}_3$ ) (ppm):  $\delta$  9.44 (s, 1H), 7.51 (s, 2H), 7.25 (s, 2H), 7.02 (s, 1H), 2.95 (s, 2H), 2.55 (d,  $J$  = 1.2 Hz, 4H), 1.57 (s, 1H), 1.42 (s, 2H), 0.86 (t,  $J$  = 7.3 Hz, 3H).

#### 4. Conclusions

In conclusion, the magnetic  $\text{Fe}_3\text{O}_4$  nanoparticles are used as catalyst in homogeneous catalytic system, and we have achieved the recovery of the catalyst by magnetic field in aza-Michael addition reaction, which is of great significance to develop the sustainable and green process of homogeneous catalytic reaction. In this catalytic system, the tedious separation procedures are replaced by an external magnetic field, which gives a different direction for picking a catalyst inhomogeneous catalysis. The magnetic  $\text{Fe}_3\text{O}_4$  nanoparticles-based catalyst gives excellent yields at room temperature, and both primary amine and secondary amine can react with various acryl amides providing a good output to target products successfully. Further experiments reveal that the catalyst can be recycled 10 times, and also maintains a high catalytic activity. Meanwhile, this study in catalytic applications may be useful in the selection and design of a catalytic system with novel selectivity and activity in an even broader range of chemical reactions.

**Supplementary Materials:** The following are available online at [www.mdpi.com/2073-4344/7/7/219/s1](http://www.mdpi.com/2073-4344/7/7/219/s1), Figure S1: TEM image of the recyclable  $\text{Fe}_3\text{O}_4$  nanoparticles, Figure S2: Wide-angle X-ray diffraction pattern of the recyclable  $\text{Fe}_3\text{O}_4$  nanoparticles and NMR spectra for all aza-Michael addition products.

**Acknowledgments:** We gratefully acknowledge the financial support from the National Natural Science Foundation of China (NSFC) (Grant Nos. 21501197) and Science Foundation of China University of Petroleum, Beijing (Grant No. 2462015YJRC004).

**Author Contributions:** Z.-X.L. and H.X. conceived and designed the experiments; D.L. and M.-M.L. performed the experiments; X.-F.X. analyzed the data; Z.-Z.M. contributed reagents/materials/analysis tools; Z.-X.L. wrote the paper.

**Conflicts of Interest:** The authors declare no conflict of interest.

## References

1. De Jesús, E.; Flores, J.C. Dendrimers: Solutions for catalyst separation and recycling—A review. *Ind. Eng. Chem. Res.* **2008**, *47*, 7968–7981. [[CrossRef](#)]
2. Astruc, D.; Lu, D.F.; Aranzaes, J.R. Nanoparticles as recyclable catalysts: The frontier between homogeneous and heterogeneous catalysis. *Angew. Chem. Int. Ed.* **2005**, *44*, 7852–7872. [[CrossRef](#)] [[PubMed](#)]
3. Lun, X.; Liebscher, J. Carbon-carbon coupling reactions catalyzed by heterogeneous palladium catalysts. *Chem. Rev.* **2007**, *107*, 133–173.
4. Köhler, K.; Heidenreich, R.G.; Krauter, J.G.E.; Pietsch, J. Highly active palladium/activated carbon catalysts for heck reactions: Correlation of activity, catalyst properties, and Pd leaching. *Chem. Eur. J.* **2002**, *8*, 622–631. [[CrossRef](#)]
5. Yu, J.; Shen, A.; Cao, Y.; Lu, G. Preparation of Pd-Diimine@SBA-15 and its catalytic performance for the Suzuki coupling reaction. *Catalysts* **2016**, *6*, 181. [[CrossRef](#)]
6. Mehnert, C.P.; Weaver, D.W.; Ying, J.Y. Heterogeneous Heck catalysis with palladium-grafted molecular sieves. *J. Am. Chem. Soc.* **1998**, *120*, 12289–12296. [[CrossRef](#)]
7. Stevens, P.D.; Li, G.F.; Fan, J.D.; Yen, M.; Gao, Y. Recycling of homogeneous Pd catalysts using superparamagnetic nanoparticles as novel soluble supports for Suzuki, Heck, and Sonogashira cross-coupling reactions. *Chem. Commun.* **2005**, 4435–4437. [[CrossRef](#)] [[PubMed](#)]
8. Papp, A.; Galbacs, G.; Molnar, R. Recyclable ligand-free mesoporous heterogeneous Pd catalysts for Heck coupling. *Tetrahedron Lett.* **2005**, *46*, 7725–7728. [[CrossRef](#)]
9. Wight, A.P.; Davis, M.E. Design and preparation of organic–inorganic hybrid catalysts. *Chem. Rev.* **2002**, *102*, 3589–3613. [[CrossRef](#)] [[PubMed](#)]
10. Li, H.X.; Chai, W.; Zhang, F.; Chen, J. Water-medium Ullmann reaction over a highly active and selective Pd/Ph-SBA-15 catalyst. *Green Chem.* **2007**, *9*, 1223–1228. [[CrossRef](#)]
11. Crudden, C.M.; Sateesh, M.; Lewis, R. Mercaptopropyl-modified mesoporous silica: A remarkable support for the preparation of a reusable, heterogeneous palladium catalyst for coupling reactions. *J. Am. Chem. Soc.* **2005**, *127*, 10045–10050. [[CrossRef](#)] [[PubMed](#)]
12. Prockl, S.S.; Kleist, W.; Gruber, M.A.; Kohler, K. In situ generation of highly active dissolved palladium species from solid catalysts—A concept for the activation of aryl chlorides in the Heck reaction. *Angew. Chem. Int. Ed.* **2004**, *43*, 1881–1882. [[CrossRef](#)] [[PubMed](#)]
13. Karimi, B.; Enders, D. New N-heterocyclic carbene palladium complex/ionic liquid matrix immobilized on silica: Application as recoverable catalyst for the Heck reaction. *Org. Lett.* **2006**, *8*, 1237–1240. [[CrossRef](#)] [[PubMed](#)]
14. Reetz, M.T.; de Vries, J.G. Ligand-free Heck reactions using low Pd-loading. *Chem. Commun.* **2004**, 35, 1559–1563. [[CrossRef](#)] [[PubMed](#)]
15. Wang, S.; Zhao, Q.; Wei, H.; Wang, J.; Cho, M.; Cho, H.; Terasaki, O.; Wan, Y. Aggregation-free gold nanoparticles in ordered mesoporous carbons: Toward highly active and stable heterogeneous catalysts. *J. Am. Chem. Soc.* **2013**, *135*, 11849–11860. [[CrossRef](#)] [[PubMed](#)]
16. Sydnes, M.O. The Use of palladium on magnetic support as catalyst for Suzuki–Miyaura cross-coupling reactions. *Catalysts* **2017**, *7*, 35. [[CrossRef](#)]
17. Carretin, S.; Blanco, M.C.; Corma, A.; Hashmi, A.S. K. Heterogeneous gold-catalysed synthesis of phenols. *Adv. Synth. Catal.* **2006**, *348*, 1283–1288. [[CrossRef](#)]
18. Witham, C.A.; Huang, W.; Tsung, C.K.; Kuhn, J.N.; Somorjai, G.A.; Toste, F.D. Converting homogeneous to heterogeneous in electrophilic catalysis using monodisperse metal nanoparticles. *Nat. Chem.* **2010**, *2*, 36–41. [[CrossRef](#)] [[PubMed](#)]
19. Wan, Y.; Wang, H.; Zhao, Q.; Klingstedt, M.; Terasaki, O.; Zhao, D. Ordered mesoporous Pd/silica—Carbon as a highly active heterogeneous catalyst for coupling reaction of chlorobenzene in aqueous media. *J. Am. Chem. Soc.* **2009**, *131*, 4541–4550. [[CrossRef](#)] [[PubMed](#)]

20. Gaikwad, A.V.; Holuigue, A.; Thathagar, M.B.; ten Elshofand, E.; Rothenberg, G. Ion- and atom-leaching mechanisms from palladium nanoparticles in cross-coupling reactions. *Chem. Eur. J.* **2007**, *13*, 6908–6913. [[CrossRef](#)] [[PubMed](#)]
21. Li, Z.X.; Xue, W.; Guan, B.T.; Shi, F.B.; Shi, Z.J.; Jiang, H.; Yan, C.H. A conceptual translation of homogeneous catalysis into heterogeneous catalysis: Homogeneous-like heterogeneous gold nanoparticle catalyst induced by ceria supporter. *Nanoscale* **2013**, *5*, 1213–1220. [[CrossRef](#)] [[PubMed](#)]
22. Perlmutter, P. *Conjugate Addition Reactions in Organic Synthesis*; Pergamon: Oxford, UK, 1992.
23. Nising, C.F.; Bräse, S. Recent developments in the field of oxa-Michael reactions. *Chem. Soc. Rev.* **2012**, *41*, 988–999. [[CrossRef](#)] [[PubMed](#)]
24. Nising, C.F.; Bräse, S. The oxa-Michael reaction: From recent developments to applications in natural product synthesis. *Chem. Soc. Rev.* **2008**, *37*, 1218–1228. [[CrossRef](#)] [[PubMed](#)]
25. Vaxelaire, C.; Winter, P.; Christmann, M. One-pot reactions accelerate the synthesis of active pharmaceutical ingredients. *Angew. Chem. Int. Ed.* **2011**, *50*, 3605–3637. [[CrossRef](#)] [[PubMed](#)]
26. Busacca, C.A.; Fandrick, D.R.; Song, J.J.; Senanayake, C.H. The growing impact of catalysis in the pharmaceutical industry. *Adv. Synth. Catal.* **2011**, *353*, 1825–1864. [[CrossRef](#)]
27. Harrison, C.L.; Krawiec, M.; Forslund, R.E.; Nugent, W.A. Beyond the chiral pool: A general approach to  $\beta$ -amino- $\alpha$ -keto amides. *Tetrahedron* **2011**, *67*, 41–47. [[CrossRef](#)]
28. Ying, A.; Li, Z.; Yang, J.; Liu, S.; Xu, S.; Yan, H.; Wu, C. DABCO-based ionic liquids: Recyclable catalysts for aza-Michael addition of  $\alpha,\beta$ -unsaturated amides under solvent-free conditions. *J. Org. Chem.* **2014**, *79*, 6510–6516. [[CrossRef](#)] [[PubMed](#)]
29. Corey, E.J.; Reichard, G.A. Enantioselective and practical syntheses of R- and S-fluoxetine. *Tetrahedron Lett.* **1989**, *30*, 5207–5210. [[CrossRef](#)]
30. Duan, J.; Li, P. Asymmetric organocatalysis mediated by primary amines derived from cinchona alkaloids: Recent advances. *Catal. Sci. Technol.* **2014**, *4*, 311–320. [[CrossRef](#)]
31. Schmidt, R.R.; Vankar, Y.D. 2-Nitroglycals as powerful glycosyl donors: Application in the synthesis of biologically important molecules. *Acc. Chem. Res.* **2008**, *41*, 1059–1073. [[CrossRef](#)] [[PubMed](#)]
32. Fabris, M.; Lucchini, V.; Noe, M.; Perosa, A. Ionic liquids made with dimethyl carbonate: Solvents as well as boosted basic catalysts for the Michael reaction. *Chem. Eur. J.* **2009**, *15*, 12273–12282. [[CrossRef](#)] [[PubMed](#)]
33. Stewart, I.C.; Bergman, R.G.; Toste, F.D. Phosphine-catalyzed hydration and hydroalkoxylation of activated olefins: Use of a strong nucleophile to generate a strong base. *J. Am. Chem. Soc.* **2003**, *125*, 8696–8697. [[CrossRef](#)] [[PubMed](#)]
34. Kisanga, P.B.; Illankumaran, P.; Fetterley, B.M.; Verkade, J.G.  $P(RNCH_2CH_2)_3N$ : Efficient 1,4-addition catalysts. *J. Org. Chem.* **2002**, *67*, 3555–3560. [[CrossRef](#)] [[PubMed](#)]
35. Sun, S.; Zeng, H.; Robinson, D.B.; Raoux, S.; Rice, P.M.; Wang, S.X.; Li, G. Monodisperse  $MFe_2O_4$  ( $M = Fe, Co, Mn$ ) nanoparticles. *J. Am. Chem. Soc.* **2004**, *126*, 273–279. [[CrossRef](#)] [[PubMed](#)]
36. Zeng, H.; Rice, P.M.; Wang, S.X.; Sun, S. Shape-controlled synthesis and shape-induced texture of  $MnFe_2O_4$  nanoparticles. *J. Am. Chem. Soc.* **2004**, *126*, 11458–11459. [[CrossRef](#)] [[PubMed](#)]
37. Tirosh, E.; Shemer, G.; Markovich, G.; Markovich, G. Optimizing cobalt ferrite nanocrystal synthesis using a magneto-optical probe. *Chem. Mater.* **2006**, *18*, 465–470. [[CrossRef](#)]
38. Bao, N.; Shen, L.; Wang, Y.; Padhan, P.; Gupta, A. A facile thermolysis route to monodisperse ferrite nanocrystals. *J. Am. Chem. Soc.* **2007**, *129*, 12374–12375. [[CrossRef](#)] [[PubMed](#)]
39. Song, Q.; Zhang, Z.J. Shape control and associated magnetic properties of spinel cobalt ferrite nanocrystals. *J. Am. Chem. Soc.* **2004**, *126*, 6164–6168. [[CrossRef](#)] [[PubMed](#)]
40. Vestal, C.R.; Song, Q.; Zhang, Z.J. Effects of interparticle interactions upon the magnetic properties of  $CoFe_2O_4$  and  $MnFe_2O_4$  nanocrystals. *J. Phys. Chem. B* **2004**, *108*, 18222–18227. [[CrossRef](#)]
41. Xu, D.Q.; Luo, S.P.; Wang, Y.F.; Xia, A.B.; Yue, H.D.; Wang, L.P.; Xu, Z.Y. Organocatalysts wrapped around by Poly(ethylene glycol)s (PEGs): A unique host–guest system for asymmetric Michael addition reactions. *Chem. Commun.* **2007**, 4393–4395. [[CrossRef](#)] [[PubMed](#)]
42. Choudhary, V.R.; Dumbre, D.K.; Patil, S.K.  $FeCl_3$ /montmorillonite K10 as an efficient catalyst for solvent-free aza-Michael reaction between amine and  $\alpha,\beta$ -unsaturated compounds. *RSC Adv.* **2012**, *2*, 7061–7065. [[CrossRef](#)]

43. Yang, L.; Xu, L.W.; Xia, C.G. Highly efficient  $\text{KF}/\text{Al}_2\text{O}_3$ -catalyzed versatile hetero-Michael addition of nitrogen, oxygen, and sulfur nucleophiles to  $\alpha,\beta$ -ethylenic compounds. *Tetrahedron Lett.* **2005**, *46*, 3279–3282. [[CrossRef](#)]
44. Surendra, K.; Krishnaveni, N.S.; Sridhar, R.; Rao, K.R.  $\beta$ -Cyclodextrin promoted aza-Michael addition of amines to conjugated alkenes in water. *Tetrahedron Lett.* **2006**, *47*, 2125–2127. [[CrossRef](#)]
45. Perin, G.; Borges, E.L.; Rosa, P.C.; Carvalho, P.N.; Lenardão, E.J. Simple cleavage of diorganyl diselenides with  $\text{NaBH}_4/\text{PEG-400}$  and direct Michael addition to electron-deficient alkenes. *Tetrahedron Lett.* **2013**, *54*, 1718–1721. [[CrossRef](#)]
46. Wang, X.; Quan, Z.; Zhang, Z. Michael additions of dihydropyrimidines and 2-amino-1,3,4-thiadiazoles to  $\alpha,\beta$ -ethylenic compounds: Using polyethylene glycols as a green reaction media. *Tetrahedron* **2007**, *63*, 8227–8233. [[CrossRef](#)]
47. Alleti, R.; Woon, S.O.; Perambuduru, M.; Ramena, C.V.; Reddy, V.P. Imidazolium-based polymer supported gadolinium triflate as a heterogeneous recyclable Lewis acid catalyst for Michael additions. *Tetrahedron Lett.* **2008**, *49*, 3466–3470. [[CrossRef](#)]
48. Jin, J.; Oskam, P.C.; Karmee, S.K.; Straathof, A.J.; Hanefeld, U. MhyADH catalysed Michael addition of water and in situ oxidation. *Chem. Commun.* **2010**, *46*, 8588–8590. [[CrossRef](#)] [[PubMed](#)]
49. Cai, J.F.; Guan, Z.; He, Y.H. The lipase-catalyzed asymmetric C–C Michael addition. *J. Mol. Catal. B Enzym.* **2011**, *68*, 240–244. [[CrossRef](#)]
50. Madalińska, L.; Kwiatkowska, M.; Cierpień, T.; Kiełbasiński, P. Investigations on enzyme catalytic promiscuity: The first attempts at a hydrolytic enzyme-promoted conjugate addition of nucleophiles to  $\alpha,\beta$ -unsaturated sulfinyl acceptors. *J. Mol. Catal. B Enzym.* **2012**, *81*, 25–30. [[CrossRef](#)]
51. Ying, A.; Liu, S.; Ni, Y.; Qiu, F.; Xu, S.; Tang, W. Ionic tagged DABCO grafted on magnetic nanoparticles: A water-compatible catalyst for the aqueous aza-Michael addition of amines to  $\alpha,\beta$ -unsaturated amides. *Catal. Sci. Technol.* **2014**, *4*, 2115–2125. [[CrossRef](#)]



© 2017 by the authors. Licensee MDPI, Basel, Switzerland. This article is an open access article distributed under the terms and conditions of the Creative Commons Attribution (CC BY) license (<http://creativecommons.org/licenses/by/4.0/>).